ISSN 1392 - 1207. MECHANIKA. 2009. Nr. 4(78)

Comparison of dynamic behaviour of EMA-3 railgun under differently induced loadings

L. Tumonis*, M. Schneider, R. Kačianauskas***, A. Kačeniauskas******

**Vilnius Gediminas Technical University, Saulėtekio 11, 10223 Vilnius, Lithuania, E-mail: liudas.tumonis@fm.vgtu.lt*
***French-German Research Institute of Saint Louis (ISL), 5 rue G'al Cassagnou, 68301 Saint-Louis, France, E-mail: schneider_m@isl.tm.fr*
****Vilnius Gediminas Technical University, Saulėtekio 11, 10223 Vilnius, Lithuania, E-mail: rkac@fm.vtu.lt*
*****Vilnius Gediminas Technical University, Saulėtekio 11, 10223 Vilnius, Lithuania, E-mail: arnka@fm.vtu.lt*

1. Introduction

The railgun is a mechatronic system used to accelerate projectiles up to very high velocities (> 2 km/s) and their great technical applications can be expected during next decade. The accelerations needed to attain these velocities, however, demand high currents generating high magnetic fields and very large Lorentz forces acting on the projectile and rails. A typical gun is composed of two rails, the projectile including a conducting armature and an energy source closes the electric circuit. The rails guide the projectile and provide current to the armature in the projectile. Experimentally realized railgun systems differ with respect to structure of rails and housing [1-5].

Enormous current densities, heat generation, high velocities and friction forces coupled with the dynamical interaction at the rail surface present a great challenge to all scientists working in this interdisciplinary research area. On the basis of existing practice one can conclude that fundamental theoretical issues have been solved and several electromagnetic railgun systems have been designed [6].

Dynamic deformation behaviour is an important component of railgun physics. The question concerning characterisation of the particular railgun systems in terms of technical parameters is, however, still open and many details require careful examination. As in the case of classical guns, the mechanical response of the housing to the transient loading (magnetic pressure) may lead to disturbances of the projectile trajectory due to momentum transfer. Additionally, deflections of contacting surfaces causes damage of the rails due to armature interaction and occurring high stresses. Dynamic effects, especially at velocities near the critical cause a drastic difference in the structure response [7]. Therefore, evaluation of the displacements of rail surfaces due to dynamic behaviour is a mandatory task for future systems.

Various approaches and models have been recently employed for modelling purposes. The mechanical, or structural, analysis of the railgun system can be decoupled from electromagnetic phenomena in a first step.

The next simplification concerns dynamic model is transient elastic waves in electromagnetic launchers and their influence on armature contact pressure were studied by Johnson and Moon [8]. It is still obvious that the railgun housing dynamics can also be treated as being independent from the projectile behaviour. The magnetic pressure, repelling the rails one from the other and expanding with the speed of the projectile, serves as force boundary condition for purely mechanical calculations.

Another issue concerns the structural model. Probably, the simplest model is to consider rail as one-dimensional beam on an elastic foundation. Analytical treatment of the beam under moving point loads and the simplest solutions are presented in the book by Fryba [9]. Moving loads in terms of shakedown approach applied to frames are considered in [10]. Investigation of dynamics of sandwich beam is presented in [11]. An analytical approach to investigate the dynamic response of laboratory railguns including projectile movement was developed in series of works by Tzeng [12] and Tzeng and Sun [13]. Here, the rail was modelled as cantilever beam on an elastic foundation.

Fig. 1 The ISL-railgun EMA3 railgun facility

In this paper, the mechanical behavior of the railgun EMA3 (Fig. 1) of the French-German Research institute of Saint-Louis (ISL) [14, 15] has been simulated numerically. At present time, it works on different kinds of armatures for electromagnetic rail launchers. The research on the electromagnetic launchers is continued in cooperation with the Vilnius High Magnetic Field Centre. In particular, various applications of the FEM including linear actuators [16], destructive coils [17] and railguns [18] were considered.

Dynamic behaviour of the rail in EMA3 system under uniformly distributed load moving with various velocities was studied in [19] by applying the 2D FE model resting on discrete elastic supports. It should be noted that this type of load may be regarded as simplest approximation of the real load profile. The experimentally measured loading generated by two current injections added in breech feed point was investigated in [20]. This loading regime will be termed hereafter as breech-feed or conventional loading regime.

The aim of this paper to compare mechanical behaviour of the railgun structure under two different experimentally measured loadings. The so called DES and

breech-fed are considered.

An outline of the paper is as follows. Section 2 presents the description of the railgun problem. Section 3 describes the modelling approach. Numerical results are discussed in section 4. Conclusions are drawn in section 5.

2. Problem description

2.1. Rail geometry and material data

The ISL railgun EMA3 with a length of 3 m and a calibre of 15x30 mm^2 was investigated. The particularity of the investigation is represented by the type of railgun housing. A view of the railgun cross-section is presented in Fig. 2, a. Here, all sizes are given in millimeters. In order to withstand the high forces repelling the rails from each other, the housing consists of a combination of bars with section size 160×80 mm of EPM 203 glass fibre reinforced plastic (GRP) material and discontinuous steel bolts. The housing design not only allows relatively quick mounting/dismounting but also taking flash radiographs during the acceleration phase [15]. The rails of section size 30×15 mm are made of Cu alloy (CRM 16N). Multiple brush armatures were used during the experiments.

Considering the axial symmetry of the rail, only half of its cross section can be investigated. A simplified model of the railgun structure is presented in Fig. 2, b. The model section is composite. Here, two section bolts fabricated from steel and having section area are modelled by a single rod located on the section center.

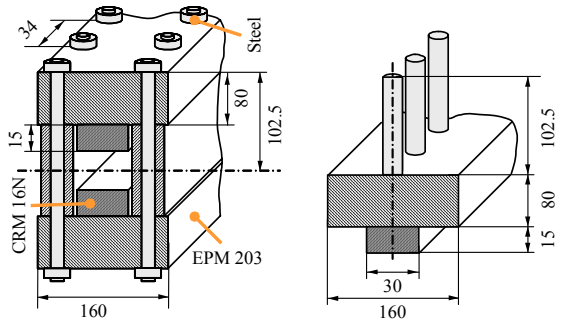

Fig. 2 Railgun structure – sectional view: a - original; b - simplified model

Material properties employed in numerical tests of the railgun are given in Table.

Table

Material properties

	Material	Physical properties
Rail	Aluminium	Density: $\rho = 2.75$ g/cm^3 Elast. modulus: $E = 69$ GPa Poisson's ratio: $\nu = 0.3$
Bolt	Steel	Density: $\rho = 8.9$ g/cm^3 Elast. modulus: $E = 207$ GPa Poisson's ratio: $\nu = 0.3$
Housing	EPM 203	Density: $\rho = 1.85$ g/cm^3 Elast. modulus: $E = 18$ GPa Poisson's ratio: $\nu = 0.3$

2.2. Moving loads

The mechanical approach introduced here considers only a simplified case of the expanding magnetic pressure volume caused by the moving projectile, while local transversal contact forces caused by the projectile (armature) are neglected. As a result, the transient loading profile represents the magnetic pressure $q(x, t)$ at an arbitrary point x moving in time t with the velocity $v(t)$.

Two types of transient loading are considered. They present so called breech-fed and DES loadings. Both loadings are generated by two current injections.

Independently on the particular type, loading variation along the direction of movement is defined in a form of the Heaviside step function $H(x)$

$$q(x,t) = p(t)H\left(x_f(t) - x\right) \tag{1}$$

where $p(x, t)$ represents magnetic pressure, distributed between zero and moving local coordinate x_f, while $x_f(t)$ represents the position of the load front (projectile) at time instant t. It can be expressed as

$$x_f(t) = \int_0^t v(\tau)d\tau \tag{2}$$

where $v(t)$ is the velocity of the projectile.

Variation of pressure $p(x, t)$ depends on the loading type. The breech-fed loading is generated by two current injections at the same current feed point A located in the breech (start) of the rails.

During the first injection the corresponding peak current is about 510 kA [14]. It results the first peak of load equal to the pressure value $p_{1max} = 88.4$ MPa which occurs at time instant $t_{1max} = 0.57$ ms.

The second injection is induced at reference time $t_{2r} = 1.32$ ms and reaches the second peak values $p_{2max} = 75.3$ MPa, at time instant $t_{2max} = 1.50$ ms. In summary, the breech load in Eq. (1)

$$p_{BR}(x,t) = p(t) \tag{3}$$

presents uniform pressure. Time variation of load is obtained from measurements and is depicted in Fig. 3, a. Three-dimensional view of the loading profile is depicted in Fig. 4, a.

The second case illustrates a DES regime. The nature of the DES pressure load is more complicated. It is characterised by combined transient pressure profiles generated in two different current injection points A and B, where A is starting point discussed earlier and B is defined by coordinate x_B=57 cm.

The pressure $p_A(t)$ (Fig. 3, a) generated by current injection in point A precisely replicates breech load until t_{2r}=1.32 ms. The pressure $p_B(t)$ generated by the additional second current injection is induced at reference time. It reaches the second peak values p_{2max}= 75.3 MPa. It could be remarked that envelope of both curves $p_A(t)$ and $p_B(t)$ coincides with load p_{BR} in Eq. (3).

Because of the difference in positions of injection points, distribution of current, and as a consequence, distribution of pressure $p_{DES}(x,t)$ on the rail surface is given by a discontinuous step function with jump at point x_B. In the

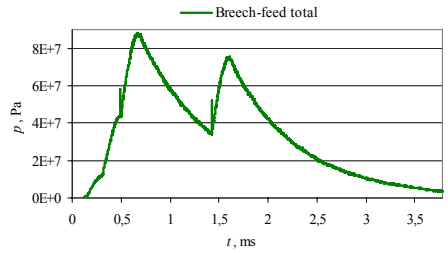

a

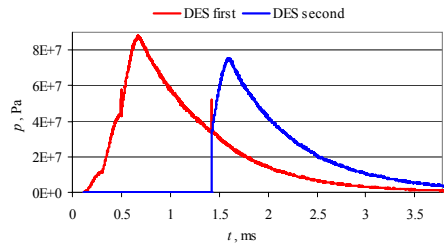

b

Fig. 3 Time variation of the pressure, acting on the rails: a - Breech-feed regime; b - DES regime

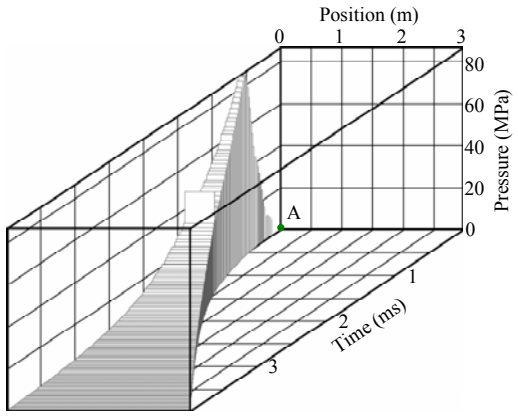

a

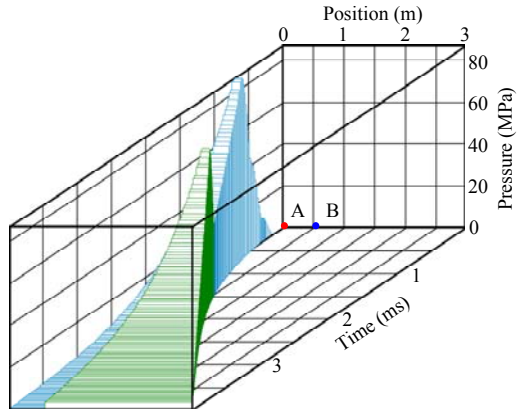

b

Fig. 4 Load variation in time A and B: a - breech-fed load; b - DES load

first segment $x < x_{B,\text{ the}}$ pressure is predefined by the first injection $p_A(t)$, while in the second segment by $x \geq x_{B,}$ by $p_B(t)$.

On this basis the DES load is defined as

$$p_{DES}(x,t) = \begin{cases} p_A(t), & \text{if } x \leq x_f(t) \text{ and if } x < x_B \\ p_B(t), & \text{if } x \leq x_f(t) \text{ and if } x \geq x_B \\ 0, & \text{if else} \end{cases}, \qquad (4)$$

Three-dimensional view of the loading profile is depicted in Fig. 4, b.

It could be provisionally observed that the main difference between both loads occurs in the first quasisegment when $x_f > x_B$. Then the breech-fed load $p_{BR}(x,t)$ according to Eq. (3) comprises pressure from two injections, while DES load $p_{DES}(x,t)$ according to Eq. (4) comprises pressure from single injection at point A. On this basis it could be realised that DES regime leads to lower load $p_{DES}(x,t) < p_{BR}(x,t)$ on the first quasisegment when projectile passes point x_B.

The respective measured velocity profile $v(t)$ of the projectile is given in Fig. 5. The artifact at about 3.5 ms is due to bad signal/noise ratio.

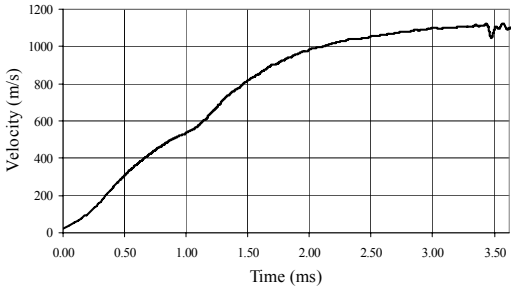

Fig. 5 Velocity profile of a projectile accelerated using EMA-3

3. Modelling Approach

The aim of the performed structural analysis has been to study an important aspect of the contact interface rail-armature, namely the displacement of the inner rail surfaces due to the magnetic pressure mentioned above.

3.1. Mathematical model

Dynamical behaviour of the rail is governed by linear mechanical model. By using matrix notations of the FEM it is written as equation of motion

$$[\boldsymbol{M}]\ddot{\boldsymbol{u}} + [\boldsymbol{K}]\boldsymbol{u} = \boldsymbol{F}_N(t) \qquad (5)$$

where, $\boldsymbol{u}$ is unknown nodal values of the time dependent displacement vector; $\ddot{\boldsymbol{u}}$ is acceleration vector; $[\boldsymbol{K}]$ is linear stiffness matrix; $[\boldsymbol{M}]$ is mass matrix; $\boldsymbol{F}_N(t)$ is prescribed vector of external time-dependent electromagnetic load. The damping term is not considered in this equation; therefore, over-estimated dynamic effects are obtained.

A 2D finite element model resting upon discrete elastic supports has been developed in order to represent the complex housing by Eq. (5). The model is able to capture bending and shear effects described conventionally by beam models as well as pinching deformation of a cross-section.

The FE model of the railgun is illustrated in Fig. 6. The rail is considered as 2D domain, while connection bolts are modelled as elastic springs. Figure shows geometry of the rail defined by length L = 3000 mm and total height h = 95 mm.

The steel bolts are transformed into 86 elastic support rods having the same length 102.5 mm. The supports are uniformly distributed along the entire rail length.

The distance between discrete supports is equal to 34 mm and approximately corresponds to the distance between the bolts. The cross-section area of the rod of 113 mm^2 presents two bolts. The supports are approximated by truss elements.

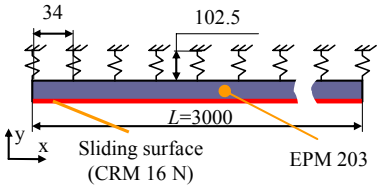

Fig. 6 2D model of the railgun

3.3. Evaluation of dynamic behaviour by averaged displacement

Solution of governing dynamic equation (5) yields time histories of the nodal displacements, while the most important issue presents local deflections of the surface under projectile.

To enhance characterisation of the railgun problem-oriented averaged displacement $\overline{u}_N$ is suggested. Actually, $\overline{u}_N$ presents average displacement of the rail surface under projectile and reflects surface deflections with position of projectile.

This parameter is obtained as integrated parameter of loaded surface as

$$\overline{u}_N\left(x_f\right)=\frac{1}{L_{proj}}\int_{x_f-L_{proj}}^{x_f}u_N dx \qquad (6)$$

here, L_{proj} is projectile length, while x_f is location of the loading front defined by Eq. (2).

Importance of the average displacement is rather two-fold. It integrates local motions of projectile-rail contact and may be regarded as reduced characteristic of the projectile. It may be attributed as characteristic of the friction [15] or gauging in the case of compression or loading efficiency of load transmission in the case of detachment.

On the other hand, the length of projectile is enough small with respect to length of the surface waves. Therefore, it appears to be proper parameter to characterize dynamics of railgun.

3.4. Numerical procedure

The numerical analysis of this mechanical model is performed by the finite element method software ANSYS [21].

The final element mesh consists of 12305 2D plane elements. The whole model includes 26911 degrees of freedom. The load is defined as normal pressure acting on the rail.

The profiles of moving load are computed in preprocessing program MOVLOAD written by using object oriented programming language C++. The resulting values of the nodal loads are stored in macro file considering native ANSYS format. The file includes information on all load steps for each time instant. Macro files are loaded by command EXECUTE MACRO finishing interactive stage of specific pre-processor MOVLOAD and FEM software ANSYS. The pre-processor automatically computes values of the nodal loads and significantly reduces time for data preparation.

The finite element modelling helped in calculation of the spring constants, visualisation of the deformation dynamics and evaluation of the deflection and stress time histories and distributions [22]

Evaluation of the average displacement (6) is implemented by postprocessor developed.

4. Numerical results and discussions

This section finally presents the results of transient analysis under two different experimentally obtained loading profiles described above.

4.1. Dynamic behaviour under breech-fed load

The conventional breech-feed loading regime is induced by a current injection in breech (start) of the rails. Its experimentally measured loading profile is depicted in Fig. 4, a. The load moves with the velocity profile shown in Fig. 5.

The two-dimensional plot of the time variation of the contact displacement is presented in Fig. 7. Here, the grey-colour scale indicates displacement magnitude. The solid line indicates path of the projectile.

It could be observed that the highest oscillation amplitudes occur at the breech of gun and the size of this region is 57 cm.

The propagation of waves is observed ahead of the projectile. Their speed is apparently higher than of the projectile and indicates pre-critical motion. Reflection and interference of waves in the end of the rail zone is also remarkable.

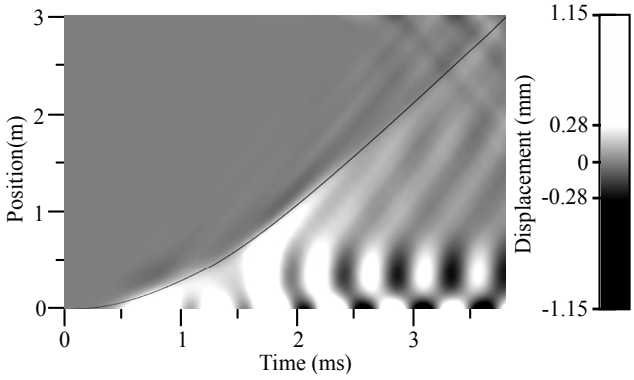

Fig. **7** Two-dimensional illustration of the time history for the breech-fed load regime

4.2. Dynamic behaviour under DES loading

The DES loading regime is depicted in Fig. 4, b. The two-dimensional plot of the time variation of the rail surface displacement is presented in Fig. 8. The graph is presented identically to the previous sample. Only the colour scale is modified for better presentation of displacements in front of the load, i.e. above the solid line.

Generally, the picture exhibits similar tendencies concerning propagation and interference of waves ahead of the projectile; however, important differences may be also detected when compared to Fig. 7. The region of the high-

est oscillation amplitudes occurred at the breech of gun is considerable smaller and is restricted by $x = 20$ cm. Maximal displacements are relatively small and may be characterised by reduction factor ~1.5.

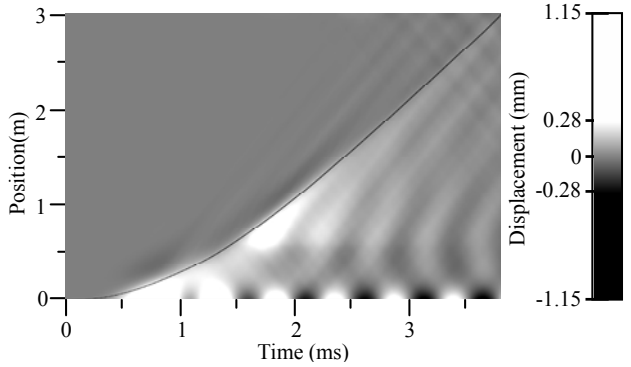

Fig. 8 Two-dimensional illustration of the time history of displacement for the DES load regime

4.3. Discussion

Two-dimensional plot of displacement profile shown in Figs. 7 and 8 can be used only for qualitative analysis. Quantitative comparison may be better completed by precise analysis of the above profiles presented in Fig. 9. Here differences $\Delta u_y(x,t) = u_{y.BR}(x,t) - u_{y.DES}(x,t)$ are exhibited in the same style.

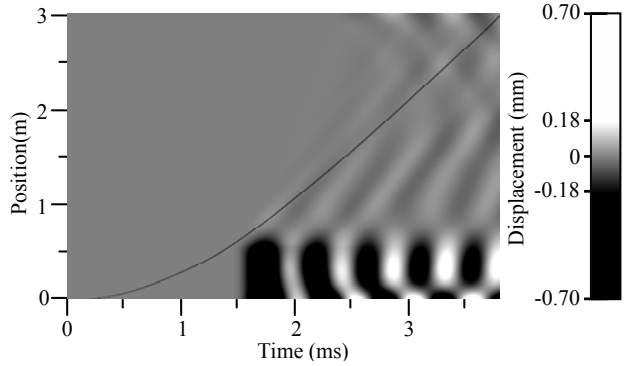

Fig. 9 Differences of two-dimensional time history of the displacement for the two loading regimes

No difference was found during the first loading phase up to 1.5 ms. The graphs only highlight, however, considerable difference of displacement near the breech. Oscillations in the start segment results differences in wave propagation ahead of the projectile.

They are attributed to the differences in the second loading stage in the DES. Increased vibrations play negative role because they reduce efficiency and durability of the system.

A detailed view of railgun surface profile at two-time instants $t = 1.89$ ms and $t = 3.78$ ms is shown in Fig. 10. It should be explained that the graph shows the displacements in $t = 0.57$ ms after occurrence of the second loading peak and responds to location of the projectile center $x_{c.proj} = 0.943$ m. It could be clearly shown that the second injection in case of the breech-fed load deforms the rail to more than two-fold of displacement amplitudes if compared to the conventional loading.

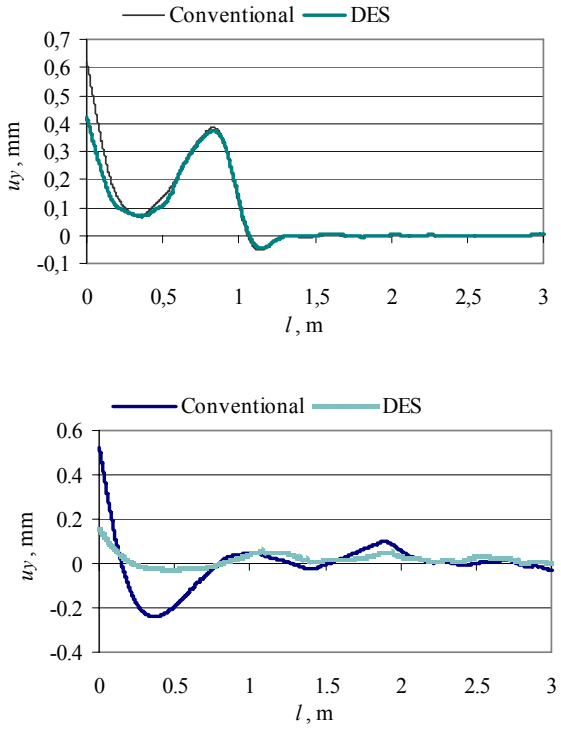

Fig. 10 Rail gun surface profiles at time instants $t = 1.89$ ms and $t = 3.78$ ms

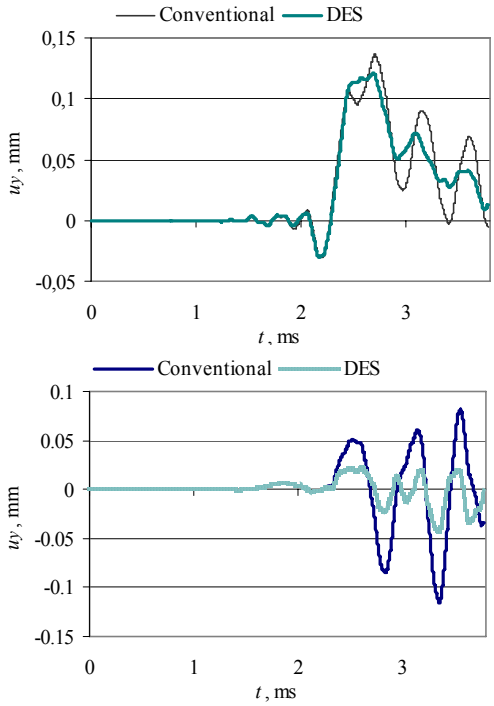

Fig. 11 Time histories of the rail surface displacements in mid-point $x = 1.5$ m and $x = 3.0$ m

The time histories of the rail middle point ($x = 1.5$ m) and $x = 3.0$ m for two different loading regimes are shown in Fig. 11. The graph shows maximum displacements 0.126 mm at time instant $t = 2.6$ ms are reached in front of the projectile located in $x_{c.proj} = 1.640$ m.

The rail deformations play a very important role at the (electrical) contact zones between the rail and armatures. This effect is evaluated by the average displacement magnitude defined by Eq. (4). Time history of the average

displacement presents time variation of average displacement of the rail contact area with the projectile. The above variation is presented in Fig. 12.

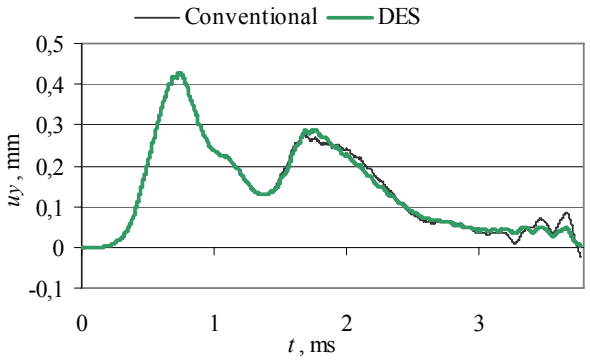

Fig. 12 Time histories of the average amplitude under projectile

It could be emphasised that both loadings yield the similar muzzle velocities lying in the range of 1200 m/s. It indicates that both loadings even the second regimes are precriticall loadings because the velocities are bellow the critical velocity 1450 m/s exhibited by the authors in [19, 20].

5. Concluding remarks

Simulation results presented qualitatively and quantitatively illustrate the differences between two different loadings which may be confirmed as follows:

- differences in breech feed and DES loadings are reflected by different dynamic behaviours in the second loading stage beginning at time instant $t = 1.6$ ms;
- the breech feed loading leads to higher oscillations of the contact surface intensified in the final stage;
- the highest amplitudes at launch end reach 0.07 mm for breech feed loading and up to 0.04 mm for DES loading.

In spite of these differences, in both cases, dynamic parameter of railgun shot is practically predetermined by the identical muzzle velocities. Since velocities are identical, it could be concluded, that DES regime is more effective and has minor influence to behaviour of the projectile. As a result, DES regime is recommended.

References

1. **Shvetsov, G., Rutberg, P., Budin**, **A.** Overview of some recent EML research in Russia. -IEEE Transactions on Magnetics, January 2007, v.43(1), p.99-106.
2. **Ross, D.P., Ferrentino, G.L.** Experimental determination of contact friction for an electromagnetically accelerated armature. -Wear, 1982, 78, p.189-200.
3. **Craddock, W., Virostek, S., Calvin H., Eljes Y.** Thermal analysis of fiber armatures. -IEEE Transactions on Magnetics, 1989, No25(1), p.127-132.
4. **Aigner, S. Igenbergs, E.** Friction and ablation measurements in a round bore railgun. -IEEE Transactions on Magnetics, 1989, No25(1), p.33-39.
5. **Lehmann, P., Peter, H., Wey, J.** Experimental study of solid armatures for EML applications. -IEEE Transactions on Magnetics, 1993, No29(1), p. 848-852.
6. **Gallant, J., Lehmann, P.** Experiments with brush projectiles in a parallel augmented railgun. -IEEE Transactions on Magnetics, 2005, No41(1), p.188-193.
7. **Daneshjoo, K., Rahimzadeh, M., Ahmadi, R., Ghassemi, M.** Dynamic response and armature critical velocity studies in an electromagnetic railgun. -IEEE Transactions on Magnetics, 2007, v.43(1), p.136-131.
8. **Johnson, A.J., Moon, F.C.** Elastic waves and solid armature contact in electromagnetic launchers. -IEEE Transactions on Magnetics, 2006, No42(3), p.422-429.
9. **Fryba, L.** Vibration of solids and structures under moving loads. -London, the UK: Thomas Telford, 1999, p. 44-56.
10. **Atkočiūnas, J., Merkevičiūtė, A., Venskus, A., Skaržauskas, V.** Nonlinear programming and optimal shakedown design of frames. -Mechanika. -Kaunas: Technologija, 2007, Nr.2(64), p.27-33.
11. **Vaičaitis, R., Liu, S., Jotautienė, E.** Nonlinear random vibrations of a sandwich beam adaptive to electrorheological materials. -Mechanika. -Kaunas: Technologija, 2008, Nr.3(71), p.38-44.
12. **Tzeng, J.T.** Structural mechanics for electromagnetic railguns, -IEEE Transactions on Magnetics, 2005, No41(1), p.246-250.
13. **Tzeng, J.T., Sun, W.** Dynamic response of cantilevered railguns attributed to projectile/gun interaction – theory, -IEEE Transactions on Magnetics, 2007, v.43(1), p.207-213.
14. **Schneider, M., Eckenfels, D., Hatterer, F.** Transition in brush armatures. -IEEE Transactions on Magnetics, 2003, v.39(1), p.76-81.
15. **Schneider, M., Schneider, R.** Sliding contact performance of multiple brush armatures. -IEEE Transactions on Magnetics, 2005, v.41(1), p.432-436.
16. **Novickij, J., Stankevič, V., Balevičius, S., Žurauskienė, N., Cimmperman, P., Kačianauskas, R., Stupak, E., Kačeniauskas, A., Löffler, M.J.** Manganite sensor for measurements of magnetic field disturbances of pulsed actuators. -Solid State Phenomena, 2006, v.113, p.459-464.
17. **Novickij, J., V., Balevičius, S., Žurauskienė, N., Kačianauskas, R., Stupak, E., Kačeniauskas, A.** Destrucctive coils. -Acta Physica Polonica, 2009, (in press).
18. **Tumonis, L., Kačianauskas, R., Kačeniauskas, A.** Evaluation of friction due to deformed behaviour of rail in the electromagnetic railgun: numerical investigation. -Mechanika -Kaunas: Technologija, 2007, Nr.1(63), p.58-63.
19. **Tumonis, L., Kačianauskas, R., Kačeniauskas, A., Schneider, M.** The transient behaviour of rails used in electromagnetic railguns: numerical investigations at constant loading velocities. -Journal of vibroengineering, 2007, v.9(3), p.15-17.
20. **Tumonis, L., Schneider, M., Kačianauskas, R., Kačeniauskas, A.** Structural mechanics of railguns in the case of discrete supports.-IEEE Transactions On Magnetics, 2009, v.45(1), p.474-479.
21. ANSYS Theory Reference, 8th edition, SAS IP INC., 2003.
22. **Lewis, K.B., Nechitailo, N.V.** Transient resonant dynamics of components in hypervelocity launchers at critical speeds. -IEEE Transactions on Magnetics, 2007, v.43(1), p.157-162.

L. Tumonis, M. Schneider, R. Kačianauskas,
A. Kačeniauskas

ELEKTROMAGNETINĖS ŠAUDYKLĖS „EMA-3" SKIRTINGŲ APKROVOS REŽIMŲ ĮTAKOS BĖGIO DINAMINIAM BŪVIUI PALYGINIMAS

R e z i u m ė

Lyginama Prancūzijos ir Vokietijos tyrimų instituto elektromagnetinės šaudyklės „EMA-3" dinamika veikiant skirtingai indukuojamoms apkrovoms. Abi magnetinio slėgio apkrovos sukeliamos dviem elektros srovės pliūpsniais ir leidžia pasiekti iki 1200 m/s kulkos greitį. Esminis skirtumas tarp apkrovų atsiranda dėl skirtingų srovės tiekimo taškų.

Modeliavimo baigtinių elementų metodu rezultatai apibūdinami slydimo plokštumos įlinkiais ir parodo skirtingą abiejų apkrovų poveikį bėgio dinaminei elgsenai. Pirmoji apkrova, susidaranti tiekiant srovę dviem pliūpsniais bėgio pradžioje, sukelia sąlygiškai didesnes bėgio paviršiaus įlinkių svyravimų amplitudes. Skaičiavimais nustatyta, kad šaudyklė yra ne tokia jautri paskirstyto energijos tiekimo režimui, kai apkrova indukuojama srovės pliūpsniais dviejose skirtinguose bėgio vietose.

L. Tumonis, M. Schneider, R. Kačianauskas,
A. Kačeniauskas

COMPARISON OF DYNAMIC BEHAVIOUR OF EMA-3 RAILGUN UNDER DIFFERENTLY INDUCED LOADINGS

S u m m a r y

Comparison of dynamic behaviour of EMA-3 railgun of the French-German Research institute of Saint-Louis (ISL) under differently induced loadings is presented. Both magnetic pressure loads are generated by two current injections and lead to identical projectile velocities reaching up to 1200 m/s. The main difference between the loads lays in different locations of the injection points.

FE simulation results presented in terms of deflections of the sliding rail surface illustrate, that loading differences result into different dynamic behaviours of the railgun. The breech-feed loading, where both injections are induced in the start position of the rail, leads to higher oscillation amplitudes of rail deflections. It was found, that the railgun structure is dynamically less sensitive to the distributed (DES) loading, induced in two different points.

Л. Тумонис, М. Шнейдер, Р. Качянаускас,
А. Каченяускас

СРАВНИВАНИЕ ДИНАМИЧЕСКОГО ПОВЕДЕНИЯ КОНСТРУКЦИИ РЕЛЬСОВОЙ ПУШКИ «ЭМА-3» ПОД ДЕЙСТВИЕМ РАЗНООБРАЗНЫХ НАГРУЗОК

Р е з ю м е

Сравнивается динамическое поведение конструкции рельсовой пушки «ЭМА-3», установленной в франсуско-немецком исследовательским институте ISL, под действием разнообразных нагрузок. Обе нагрузки индуктируются двумя импульсами тока и позволяют достичь скорость пули до 1200 м/с. Фундаментальное различие между теми нагрузками возникает из-за различия точек подачи тока.

Представленные результаты расчетов конечно-элементного метода перемещений поверхности рельса показывают различное влияние нагрузок. Первая нагрузка индуктируется двумя импульсами тока в той же самой точке в начале рельса. Установлено, что перемещения рельсовой пушки являются менее чувствительными к режиму нагрузки, если нагрузка индуктируется двумя импульсами тока в двух разных точках рельса.

Received June 10, 2009
Accepted August 21, 2009

DOI: 10.5755/j02.mech.15282